EFFICIENT AND ROBUST IMAGE SEGMENTATION WITH A NEW PIECEWISE-SMOOTH DECOMPOSITION MODEL

Ying Gu[†]*, Li-Lian Wang*[‡]*,Wei Xiong*[†]*, Jierong Cheng*[†]*,Weimin Huang*[†]*, Jiayin Zhou*[†]

[†] Institute for Infocomm Research, [‡] Nanyang Technological University

ABSTRACT

Image segmentation is to separate the image domain into local regions. Implicit active contour models via the level-set method can provide smooth and closed contours. The major category is based on the Mumford-Shah image component decomposition model. Approximating the image domain by a set of homogeneous regions, segmentation based on the piecewise constant (PC) models fail in intensity inhomogeneous images. Requiring intensity smoothness in local regions, segmentation based on the piecewise smooth (PS) models can perform better for intensity inhomogeneity than those PC based. Existing PS-based techniques are inefficient and not robust to complicate intensity scenarios with noise. Here we introduce a new functional model by decomposing an image into three parts: PS components, PC components and noise components. We convexify the decomposition model by incorporating with relaxation techniques and optimize the PS components over the whole image domain. New numerical algorithms are also proposed to implement the above approaches efficiently. Numerical validation experiments show that the proposed approaches can achieve much faster, more robust and more accurate image segmentation than existing arts.

Index Terms— Image segmentation, decomposition model, Smoothed Chambolle-Dual algorithm.

1. INTRODUCTION

Image segmentation, a fundamental task in image processing and computer vision, is to separate the image domain into local regions. Early segmentation techniques, like edge detection, need edge linking to form closed region contours. Implicit active contour models via the level-set method can provide smooth and closed contours automatically. The majority of such techniques is to approximate the image based on Mumford-Shah image component decomposition model. Approximating the image domain by a set of homogeneous regions, segmentation based on the piecewise constant (PC) models fail for intensity inhomogeneous images. Replacing by region piecewise smooth (PS) approximation models, one can better cope with the intensity inhomogeneity. Traditionally, the segmentation problem, as formulated by Mumford and Shah [1], can be defined as follows: given an observed image I, find a decomposition Ω_i of Ω and an optimal piecewise smooth approximation u of I, such that u varies smoothly within each Ω_i, and rapidly or discontinuously across the boundaries of Ω_i. To solve this problem, Mumford and Shah proposed the following minimization problem [1]:

$$\min_{u,\Gamma}\Big\{E_{MS}(u,\Gamma):=\mu\int_{\Omega\setminus\Gamma}|\nabla u|^2d\boldsymbol{x}+\frac{\nu}{2}\int_{\Omega}|u-I|^2d\boldsymbol{x}+|\Gamma|\Big\}, \tag{1.1}$$

where $|\Gamma|$ is the length of Γ, and $\mu,\nu>0$ are parameters to weight the terms in the functional.

While intensive research has been devoted to piecewise constant image segmentation, limited works are available for segmenting images with piecewise smooth structures. Compared with the piecewise constant case, one significant difficulty lies in how to efficiently handle the implicit coupling of the smooth approximation u and the edge set Γ. Many attempts tackle this problem from solving the smooth approximation in each subdomain (see, e.g., [2, 3, 4, 5]). One remarkable attempt by Vese and Chan [3] essentially employs the level-set method in [6] to reformulate the Mumford-Shah model, and this requires to solve the approximation $\{u_i\}$ (satisfying elliptic-type equations) within the subdomain of $\{\Omega_i\}$ (identified by the level-set functions) in the dynamical evolution of the level-set functions. However, it requires the initial curve to be close to the boundaries, otherwise the convergence of the curve to object boundary will be too slow, and for highly noisy images, it almost collapses. Indeed, with a good initialization, the proposed approach produces satisfactory segmentation results. In practice, one would expect to alleviate the dependence of u on Γ, for example, just to resolve u on the whole domain Ω.

In modeling images with intensity inhomogeneity [7, 8], the following model was proposed:

$$I(\boldsymbol{x})=b(\boldsymbol{x})c_i+n(\boldsymbol{x}),\quad \boldsymbol{x}\in\Omega_i,\ \ 1\le i\le m,$$

where Ω is the disjoint of $\{\Omega_i\}_{i=1}^m$, b is a smooth function that models the bias field (i.e., intensity inhomogeneity) in images, $\{c_i\}$ are constant intensity values, and n models the additive white Gaussian noise. One important assumption in this context is that the bias field b varies slowly and takes value around 1. In other words, the image of interest consists

of piecewise constant structures with a "small perturbation" induced by the bias field.

In this paper, we propose a new decomposition model of the image:

$$I(\boldsymbol{x}) = \lambda b(\boldsymbol{x}) + (1-\lambda)\sum_{i=1}^{m} c_i\chi_i(\boldsymbol{x}) + n(\boldsymbol{x}), \ \text{ a.e. in } \Omega, \tag{1.2}$$

where $\lambda > 0$ is a constant, and $\{\chi_i\}$ are the characteristic functions of $\{\Omega_i\}$. Note that for each i

$$\chi_i(\boldsymbol{x}) = \begin{cases} 1, & \text{if } \boldsymbol{x} \in \Omega_i, \\ 0, & \text{if } \boldsymbol{x} \in \Omega \setminus \Omega_i. \end{cases}$$

We basically view a clear image (i.e., $I - \boldsymbol{n}$) as a combination of a smooth field and piecewise constant structures. We integrate the model (1.2) with the Mumford-Shah model to coming up a robust model for multiphase piecewise smooth image segmentation. We also provide efficient algorithms for its minimization problem and show its advantages over the existing model and approach.

This paper is organized as follows. In Section 2, we introduce the model resulted from an integration of the decomposition model with the Mumford-Shah model, and present the relaxation technique. In Section 3, we present the algorithms to solve the minimization problem, consisting of the Fourier method and Smoothed Chambolle-Dual algorithm. Comparison of numerical results are presented in Section 4.

2. THE DECOMPOSITION MODEL

We first introduce the model resulted from an integration of the decomposition (1.2) with the Mumford-Shah model (1.1). We can find an approximation by solving the least-square problem and adding the total variational and regularization term. Let $\{v_i\}_{i=1}^m$ be the characteristics of $\{\Omega_i\}_{i=1}^m$. Then we adopt H^1-regularization for the smooth component and total variation regularization for the length of the edges. This leads to the energy functional:

$$\begin{aligned} E\big(b,\boldsymbol{c},\boldsymbol{v}\big) &:= \sum_{i=1}^{m}\Big(\mu\lambda^2\int_\Omega |\nabla b|^2 v_i\,d\boldsymbol{x} \\ &+ \frac{\nu}{2}\int_\Omega |I-\lambda b-(1-\lambda)c_i|^2 v_i\,d\boldsymbol{x} + \int_\Omega |\nabla v_i|\,d\boldsymbol{x}\Big), \end{aligned} \tag{2.1}$$

where $\mu, \nu, \lambda > 0$, $\boldsymbol{c} = (c_1, \cdots, c_m)$, and $\boldsymbol{v} = (v_1, \cdots, v_m)$ with

$$\boldsymbol{v} \in \mathcal{A} := \Big\{ v_i \in \{0,1\},\ \ 1 \le i \le m;\ \ \sum_{i=1}^{m} v_i \equiv 1\Big\}.$$

As $\{c_i\}$ characterize the piecewise constant structures, we would expect they return the mean of each phase, defined by

$$c_i = \frac{\int_\Omega I v_i\,d\boldsymbol{x}}{\int_\Omega v_i\,d\boldsymbol{x}}, \quad i = 1, \cdots, m. \tag{2.2}$$

It is also for convenience of implementation that we search for the triple $(b, \boldsymbol{c}, \boldsymbol{v})$ by minimizing the functional:

$$\begin{aligned} E_{PS}\big(b,\boldsymbol{c},\boldsymbol{v}\big) &:= \nu\lambda^2\int_\Omega |I-b|^2 d\boldsymbol{x} + \sum_{i=1}^{m}\Big(\int_\Omega |\nabla v_i|\,d\boldsymbol{x} \\ &+ \mu\lambda^2\int_\Omega |\nabla b|^2 v_i\,d\boldsymbol{x} + (1-\lambda)^2\nu\int_\Omega |I-c_i|^2 v_i\,d\boldsymbol{x}\Big). \end{aligned} \tag{2.3}$$

Noticing that $I = \lambda I + (1-\lambda)I$, we infer that

$$E\big(b,\boldsymbol{c},\boldsymbol{v}\big) \le E_{PS}\big(b,\boldsymbol{c},\boldsymbol{v}\big).$$

With this setup, (2.2) can be preserved.

We reiterate that one obvious challenge for minimizing (2.3) is that $\{v_i\}$ must take the binary values, so the admissible set $\mathcal{A}$ is non-convex. To minimize E_{PS}, we can relax $\mathcal{A}$ into the convex set

$$\begin{aligned} \triangle_+ :=& \Big\{\boldsymbol{v} = (v_1, \cdots, v_m) \in (BV(\Omega))^m\ : \\ & v_i \in [0,1];\ \sum_{i=1}^{m} v_i = 1\Big\}, \end{aligned}$$

where $BV(\Omega)$ is the space of bounded variation.

One can prove the existence of the minimizer of $\min_{(b,\boldsymbol{c},\boldsymbol{v})\in\Lambda_m} E_{PS}\big(b,\boldsymbol{c},\boldsymbol{v}\big)$ with the solution space:

$$\begin{aligned} \Lambda_m =& \big\{(b,\boldsymbol{c},\boldsymbol{v})\ :\ b \in H^1(\Omega);\ \boldsymbol{v} \in \triangle_+; \\ & \boldsymbol{c}\ \text{ is a constant-valued vector}\big\}. \end{aligned}$$

3. MINIMIZATION ALGORITHM

We adopt the splitting technique and seek the minimizer $(b, \boldsymbol{c}, \boldsymbol{v})$ separately as follows.

(a). Fixing $\boldsymbol{v}$ and $\boldsymbol{c}$, we search for b as a solution of

$$\min_{b\in H^1(\Omega)}\Big\{\mu\lambda^2\sum_{i=1}^{m}\int_\Omega |\nabla b|^2 v_i\,d\boldsymbol{x} + \nu\lambda^2\int_\Omega |I-b|^2 d\boldsymbol{x}\Big\}. \tag{3.1}$$

(b). Fixing $\boldsymbol{v}$ and b, we search for $\boldsymbol{c}$ as a solution of

$$\min_{\boldsymbol{c}}\Big\{\sum_{i=1}^{m}\int_\Omega |I-c_i|^2 v_i\,d\boldsymbol{x}\Big\}.$$

It is clear that the solution of $\boldsymbol{c}$ is given by (2.2) as expected.

(c). Fixing b and $\boldsymbol{c}$, we search for $\boldsymbol{v}$ as a solution of

$$\begin{aligned} \min_{\boldsymbol{v}\in\triangle_+}\Big\{\sum_{i=1}^{m}\Big(&\mu\lambda^2\int_\Omega |\nabla b|^2 v_i\,d\boldsymbol{x} \\ &+ (1-\lambda)^2\nu\int_\Omega |I-c_i|^2 v_i\,d\boldsymbol{x} + \int_\Omega |\nabla v_i|\,d\boldsymbol{x}\Big)\Big\}. \end{aligned} \tag{3.2}$$

3.1. Minimization with respect to b

Notice that for fixed c and $\boldsymbol{v}$, the function in (3.1) is convex, so it admits a unique a minimizer. The corresponding Euler-Lagrange equation of (3.1) takes the form

$$\begin{cases} -\mu \sum_{i=1}^{m} \operatorname{div}(\nabla b\, v_i) + \nu(b - I) = 0, \\ \dfrac{\partial b}{\partial \boldsymbol{n}}\Big|_{\partial\Omega} = 0, \end{cases} \tag{3.3}$$

where $\boldsymbol{n}$ is the unit outer normal vector $\partial\Omega$. To avoid solving the elliptic problem with variable coefficient, we can use a preconditioning technique (see, e.g., [9]), and Fourier methods with fast Fourier transform (FFT) to solve (3.3) very efficiently (see, e.g., [10]).

3.2. Minimization with respect to $\boldsymbol{v}$

Subproblem (3.2) can be formulated as

$$\min_{\boldsymbol{v}} \max_{\vec{\boldsymbol{p}} \in \boldsymbol{S}} \Big\{ \sum_{i=1}^{m} \int_{\Omega} v_i f_i \, d\boldsymbol{x} + \sum_{i=1}^{m} \int_{\Omega} v_i \operatorname{div} \boldsymbol{p}_i \, d\boldsymbol{x} \Big\}, \tag{3.4}$$

where

$$f_i = \mu\lambda^2 |\nabla b|^2 + (1-\lambda)^2 \nu |I - c_i|^2,$$

and $\vec{\boldsymbol{p}} = (\boldsymbol{p}_1, \boldsymbol{p}_2, \cdots, \boldsymbol{p}_m)$, $\boldsymbol{S} = S^m$ and S is defined as

$$S := \Big\{ \boldsymbol{p} = (p_1, p_2) \in C_c^1(\Omega; \mathbb{R}^2) \,:\, |\boldsymbol{p}| \le 1 \quad \forall \boldsymbol{x} \in \Omega \Big\}.$$

It is clear that (3.4) is the Potts model [11]. We have discussed the efficient implementation for the Potts model in piecewise constant case in [12]. However, this is the smooth case. The relaxation is needed to favor the smooth part in the whole domain. We use the smoothed method mentioned in [13] to change (3.4) to the smoothed model, and then use Chambolle's dual algorithm [14], which is fast and robust. We name the new efficient algorithm as Smoothed Chambolle-Dual algorithm. We next show the algorithm briefly. The smoothed model of (3.2) is equivalent to

$$\min_{\boldsymbol{v}} \max_{\vec{\boldsymbol{p}} \in \boldsymbol{S}} \int_{\Omega} \Big\{ \sum_{i=1}^{m} v_i (f_i + \operatorname{div} \boldsymbol{p}_i) \, d\boldsymbol{x} + r \sum_{i=1}^{m} v_i \log v_i d\boldsymbol{x} \Big\},$$

where r is sufficiently small. Hence we can easily obtain the expression of primal variable

$$v_i = \frac{\exp\Big(-\frac{\operatorname{div}\boldsymbol{p}_i + f_i}{r}\Big)}{\sum_{j=1}^{m} \exp\Big(-\frac{\operatorname{div}\boldsymbol{p}_j + f_j}{r}\Big)}, \quad 1 \le i \le m. \tag{3.5}$$

The corresponding dual problem is given as

$$\min_{\vec{\boldsymbol{p}} \in \boldsymbol{S}} \int_{\Omega} \Big\{ \log \sum_{i=1}^{m} \exp\Big(\frac{-f_i - \operatorname{div}\boldsymbol{p}_i}{r}\Big) \Big\} d\boldsymbol{x}. \tag{3.6}$$

Following the derivation of the Chambolle's dual algorithm [14] and (3.5), we write it the compact form of dual problem:

$$-\nabla v_i + |\nabla v_i| \boldsymbol{p}_i = 0, \quad 1 \le i \le m. \tag{3.7}$$

It can be solved by a semi-implicit discretization in time as in [14]. Let τ be the time step size and $\vec{\boldsymbol{p}}^n$ be the approximation of $\vec{\boldsymbol{p}}$ at $n\tau$. The scheme reads

$$\boldsymbol{p}_i^{n+1} = \frac{\boldsymbol{p}_i^n + \tau \nabla v_i^n}{1 + \tau |\nabla v_i^n|}, \quad 1 \le i \le m. \tag{3.8}$$

4. NUMERICAL RESULTS

In this section, we provide numerical experiments to demonstrate the performance of the decomposition model with FFT and Smoothed Chambolle-Dual (FFT-SCD) algorithm.

We first test it on the decomposition of noisy signals into piecewise constant components (obtained from $\{v_i\}$) and smooth component (contained in b), as in (1.2). For clarity and ease of understanding, we test it on the signal with piecewise constant and smooth structures, polluted by noise. We highlight in Figure 4.1 the components: $\sum c_i v_i$ (in pink), b (in black) and $u = \lambda b + (1-\lambda)\sum c_i v_i$ (in red), resulted from our model and algorithms. It is seen that even for large noise, very accurate segmentation can be obtained. Relatively, the FFT-SCD algorithm is robust for larger noise. This will be also verified by the two-dimensional tests below.

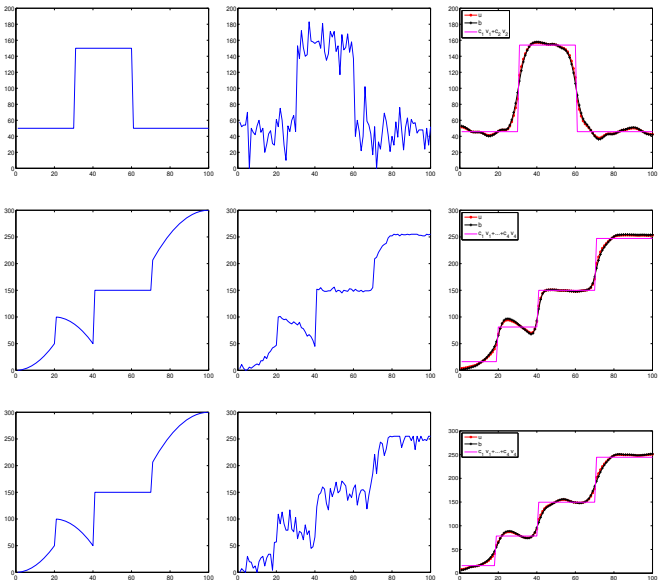

Fig. 4.1. Results obtained by FFT-SCD algorithm for one-dimensional tests with $\mu = 0.1, \nu = 0.01, \alpha = 0.01, \beta = 0.01, r = 0.1, \lambda = 0.8, \tau = 0.01$, and $\Delta t = 10^{-4}$. Column 1: the clean images; Column 2: the noisy images; Column 3: the segmented results u together with the smoothed part b and the jumps $\sum c_i v_i$ of FFT-SCD algorithm.

Next, we present in Figure 4.2 the comparison of FFT-SCD and the Vese-Chan (V-C) method [3]. We test two-phase

images with different noise levels (see, Figure 4.2(a) and Figure 4.2(d)) with different μ and ν. The results show a similar performance. We plot the segmentation results in Figure 4.2 and tabulate in Table 4.1 the computational time and evaluation results obtained by the two different algorithms. We find that FFT-SCD algorithm converges much faster and yields better segmentation than V-C method [3] (see Table 4.1).

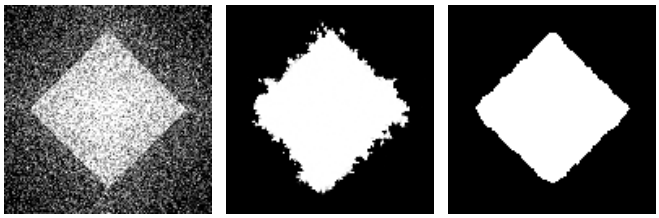

(a) Original image (b) V-C method [3] (c) FFT-SCD

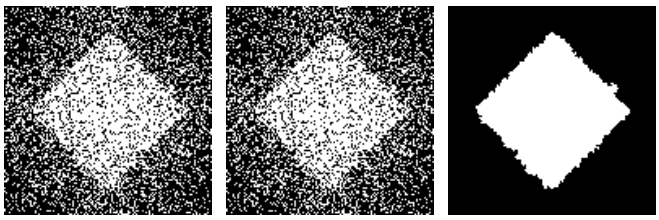

(d) Original image (e) V-C method [3] (f) FFT-SCD

Fig. 4.2. Comparison of V-C method [3] and FFT-SCD algorithm. FFT-SCD algorithm provides better results than the V-C method [3].

Table 4.1. Comparison results.

Figure 4.2(a)	time (second)	precision	recall
V-C	193.76	0.8175	0.9401
FFT-SCD	3.43	0.9890	0.9930
Figure 4.2(d)	time (second)	precision	recall
V-C	Not convergent	0.5352	0.7957
FFT-SCD	6.43	0.9640	0.9915

Finally, we test brain images in Figure 4.3(a) available to the public at "http://www.bic.mni.mcgill.ca/brainweb/". For the image used in this test the noise level is 7% and the nonuniformity intensity level of the RF-puls is 20% (see the details on the website above). There are three tissue classes that should be identified: cerebrospinal fluid, gray matter and white matter. We choose the same parameters as Figure 4.2. In Figure 4.3, we plot an example consists of the original image, segmentation results of V-C method, segmentation results of FFT-SCD algorithm, and the exact segmentation results. The performance results are compared in Table 4.2 in terms of precision and recall for each phase. Precision is the fraction of the true positive pixels in the segmented results, while recall (or sensitivity) is the fraction of the true positive pixels in the ground truth of the foreground. Table 4.2 shows that our proposed algorithm is better than V-C with larger values in both precision and recall. This is because our proposed algorithm which solve problems in the whole domain is more accurate than the V-C method which solves in each complicated subdomain.

(a) Original image (b) VC Phase 1 (c) VC Phase 2 (d) VC Phase 3

(e) Original image (f) FS Phase 1 (g) FS Phase 2 (h) FS Phase 3

(i) Original image (j) Exact-phase 1 (k) Exact-phase 2 (l) Exact-phase 3

Fig. 4.3. Results obtained by V-C method and FFT-SCD algorithm. Row 1: segmented results of V-C method. Row 1: segmented results of FFT-SCD algorithm. Row 2: exact segmented results. FFT-SCD algorithm produces comparable results as the exact results, and all these phases match the exact phases better than V-C method.

Table 4.2. Evaluation results.

	phase 1		phase 2		phase 3	
	precision	recall	precision	recall	precision	recall
V-C	0.8160	0.8501	0.7609	0.4961	0.9682	0.2131
FFT-SCD	0.9245	0.9361	0.8562	0.8753	0.8267	0.8646

5. CONCLUSION

In this paper, we introduced a new image component decomposition model for piecewise smooth image segmentation considering constant components, smooth components and noise components. We convexified the decomposition model by incorporating with relaxation techniques and optimized the approximation to smooth components over the whole image domain. We also presented new efficient numerical algorithms to implement the entire optimization for the image segmentation. The implementation of the proposed approaches does not involve complicate manipulations. These allowed us to present efficient and robust image segmentation in noisy and intensity inhomogeneous images, as compared to the counterpart of the Chambolle's algorithm. Numerical validation experiments in synthesized and multi-phase medical images with various noise levels demonstrated the advantage of the proposed approaches.

6. REFERENCES

[1] D. Mumford and J. Shah, "Optimal approximations by piecewise smooth functions and associated variational problems," *Commun. Pure Appl. Math.*, vol. 42, no. 5, pp. 577–685, 1989.

[2] A. Tsai, A.J. Yezzi, and A.S. Willsky, "Curve evolution implementation of the Mumford-Shah functional for image semgmentation, denoising interpolation, and magnification," *IEEE Trans. Image Process.*, vol. 10, no. 8, pp. 1169–1186, 2001.

[3] L.A. Vese and T.F. Chan, "A multiphase level set framework for image segmentation using the Mumford and Shah model," *Int. J. Comput. Vis.*, vol. 50, no. 3, pp. 271–293, 2002.

[4] J. Piovano, M. Rousson, and T. Papadopoulo, "Efficient segmentation of piecewise smooth images," *Proceedings of Scale Space and Variational Methods in Computer Vision*, pp. 709–720, 2007.

[5] Y. Zhang, "Fast segmentation for the piecewise smooth mumford-shah functional," *Int. J. Signal Process.*, vol. 2, no. 4, 2006.

[6] S. Osher and J.A. Sethian, "Fronts propagating with curvature dependent speed: algorithms based on hamilton-jacobi formulations," *J. Comput. Phys.*, vol. 79, no. 1, pp. 12–49, 1988.

[7] D.L. Pham and J.L. Prince, "An adaptive fuzzy c-means algorithm for the image segmentation in the presence of intensity inhomogeneities," *Pattern Recognit. Lett.*, vol. 20, no. 1, pp. 57–68, 1998.

[8] W. Wells, E. Grimson, R. Kikinis, and F. Jolesz, "Adaptive segmentation of mri data," *IEEE Trans. Med. Imag.*, vol. 15, no. 4, pp. 429–442, 1996.

[9] H. Ceniceros and T.Y. Hou, "An efficient dynamically adaptive mesh for potentially singular solutions," *J. Comput. Phys.*, vol. 172, no. 2, pp. 1–31, 2001.

[10] J. Shen, T. Tang, and L.L. Wang, *Spectral Methods: Algorithms, Analysis and Applications*, Springer, 2011.

[11] R.B. Potts, "Some generalized order-disorder transformations," in *Proceedings of the Cambridge Philosophical Society*, 1952, vol. 48, pp. 106–109.

[12] Y. Gu, L.L. Wang, and X.C. Tai, "A direct approach towards global minimization for multiphase labeling and segementation problems," *IEEE Trans. Image Process.*, vol. 21, no. 5, pp. 2399–2411, 2012.

[13] E. Bae, J. Yuan, and X.C. Tai, "Global minimization for continuous multiphase partitioning problems using a dual approach," *Int. J. Comput. Vision*, vol. 92, no. 1, pp. 112–129, 2011.

[14] A. Chambolle, "An algorithm for total variation minimization and applications," *J. Math. Imagng Vision*, vol. 20, no. 1, pp. 89–97, 2004.